



Ambient effects on electric-field-induced local charge modification of TiO₂

Haeri Kim, Seungbum Hong, and Dong-Wook Kim

Citation: [Applied Physics Letters](#) **100**, 022901 (2012); doi: 10.1063/1.3675630

View online: <http://dx.doi.org/10.1063/1.3675630>

View Table of Contents: <http://scitation.aip.org/content/aip/journal/apl/100/2?ver=pdfcov>

Published by the [AIP Publishing](#)

Articles you may be interested in

[Probing electron density across Ar⁺ irradiation-induced self-organized TiO_{2-x} nanochannels for memory application](#)

Appl. Phys. Lett. **108**, 244104 (2016); 10.1063/1.4954166

[Examination of interfacial charge transfer in photocatalysis using patterned CuO thin film deposited on TiO₂](#)

APL Mater. **3**, 104409 (2015); 10.1063/1.4926934

[Localized states induced by an oxygen vacancy in rutile TiO₂](#)

J. Appl. Phys. **117**, 225703 (2015); 10.1063/1.4922184

[Fermi level shifting of TiO₂ nanostructures during dense electronic excitation](#)

Appl. Phys. Lett. **99**, 013109 (2011); 10.1063/1.3608140

[Electrical behavior and oxygen vacancies in BiFeO₃ / \[\(Bi 1 / 2 Na 1 / 2 \) 0.94 Ba 0.06 \] TiO₃ thin film](#)

Appl. Phys. Lett. **95**, 192901 (2009); 10.1063/1.3259655

The image shows the cover of an Applied Physics Reviews journal issue. It features a blue and orange color scheme with a molecular structure background. The text 'AIP Applied Physics Reviews' is at the top left. The main title 'NEW Special Topic Sections' is in large white letters. Below it, 'NOW ONLINE' is written in orange, followed by 'Lithium Niobate Properties and Applications: Reviews of Emerging Trends' in white. The AIP Applied Physics Reviews logo is at the bottom right.

NEW Special Topic Sections

NOW ONLINE
Lithium Niobate Properties and Applications:
Reviews of Emerging Trends

AIP Applied Physics
Reviews

Ambient effects on electric-field-induced local charge modification of TiO₂

Haeri Kim,^{1,2} Seungbum Hong,^{2,a)} and Dong-Wook Kim^{1,3,a)}

¹Department of Physics, Ewha Womans University, Seoul 120-750, Korea

²Materials Science Division, Argonne National Laboratory, Lemont, Illinois 60439, USA

³Department of Chemistry and Nano Science, Ewha Womans University, Seoul 120-750, Korea

(Received 20 July 2011; accepted 6 December 2011; published online 9 January 2012)

We investigated the surface potential of TiO₂ single crystals using scanning probe microscopy (SPM) under different gas environment. The SPM tip-induced electrical stress resulted in reversal in the surface potential, V_{surf} , polarity only in H₂/Ar ($\Delta V_{\text{surf}} = 0.30$ eV) and not in Ar and O₂. Quantitative measurement of the influence of ambient gas on the surface potential led us to develop a model where the adsorbed oxygen molecules and oxygen vacancies interact to change their relative concentration leading to different surface potential in TiO₂. These results will give us insights into ambient-dependent physical phenomena in oxide thin film nanostructures. © 2012 American Institute of Physics. [doi:10.1063/1.3675630]

In metal oxides, which are quite distinct from conventional semiconductors, an alteration of the “free charge” density can cause peculiar physical phenomena, including superconducting states, metal-to-insulator transitions, and colossal magnetoresistance.^{1–3} In addition, “bound charges” induced by spontaneous polarization in polar oxides can be used as information storage units.^{4–6} In all such cases, oxygen ions (or oxygen vacancies) can play important roles because they can act as mobile dopants that directly affect the sample conductivity and screen charges that compensates for some of the net charges in the material. Furthermore, coupled electron-ion dynamics at the surface and interface of the oxides can play key roles in many of interesting physical phenomena, including resistive switching, catalytic activity, and sensing.^{7–13} Therefore, manipulating and characterizing the electric charges in these materials (electrons and ions) are crucial for investigating the intriguing physics of metal oxides. Scanning probe microscopy (SPM) is one of the best tools for these purposes because of its versatility and superior resolution compared with other techniques.^{2,3,5,6,12–14} Recently, water and carbon-containing gas adsorption on the oxide surface was claimed to significantly affect local charge modification^{2,3,13} but roles of oxidizing and reduction gases in the SPM experiments have not been explicitly investigated.

Among the numerous metal oxides, TiO₂ exhibits a variety of interesting physical properties including resistive switching⁷ and catalytic activity.^{8–11} As such there have been several efforts to identify the dominant mechanism that accounts for the charge transport and trapping in TiO₂ or at the TiO₂/metal interface.^{7–11}

Here, we conducted SPM experiments, using electrostatic force microscopy (EFM) in particular, to investigate how an SPM-tip-induced electric field influences the surface potential distribution of rutile TiO₂ (100) single crystals under various environments with different degree of oxygen partial pressure. Single crystalline samples have flat topography, negligible structural disorder, and chemical inhomogeneity, which

provide ideal platforms to study the influence of local charge injection and ambient oxygen molecules on the surface potential without concerns of artifacts coming from preferential transport paths for ions and electrons through defects or topological variations.

We used rutile TiO₂ (100) single crystals (Crystec) for the SPM measurements. The EFM measurements were performed using an SPM system with a closed fluid cell to maintain a specific gas environment (MFP-3D, Asylum Research) and Pt-coated Si cantilevers (NSG01/Pt, NT-MDT). Three different gases, H₂ (2%)/Ar (98%), Ar, and O₂, were used to control the ambient in the closed cell (see supplementary material for details¹⁵). Just prior to the SPM experiments, the TiO₂ sample was heated to 150 °C for 30 min to remove water molecules that had been adsorbed on the surface (see supplementary material for details¹⁵). The topography was obtained using AC mode with a drive frequency of 145 kHz (slightly lower than the resonance frequency of the cantilever), and EFM images of the surface were simultaneously acquired by applying an AC modulation voltage of amplitude (V_{ac}) of 3 V and a frequency (ω) of 20 kHz to the tip.⁶

Figure 1(a) shows the topographical images obtained from the three different ambient gases. The square-shaped area at the center of each image was scanned by the SPM tip with a DC bias (V_{dc}) of +10 V in contact mode. Such a tip-scanning process will be called “tip-induced stress” for the remainder of this paper. The stressed region apparently becomes higher than the surrounding (unstressed) region, and the relative height difference is dependent on the ambient gas. Tip-induced local oxidation is possible and can cause topographical change, while a negative bias voltage is applied to the SPM tip.¹² However, our experiments were carried out in a cell filled with highly pure (>99.999%) gas and under a positive tip bias, which excludes the possibility of anodization process. The apparent topographical change seems to instead have originated from the electrostatic force between the tip and the sample. (see supplementary material for details¹⁵).

The electrostatic force between the tip and the sample, F_e , consists of a capacitive force and the Coulombic interaction.

^{a)}Authors to whom correspondence should be addressed. Electronic addresses: hong@anl.gov and dwkim@ewha.ac.kr.

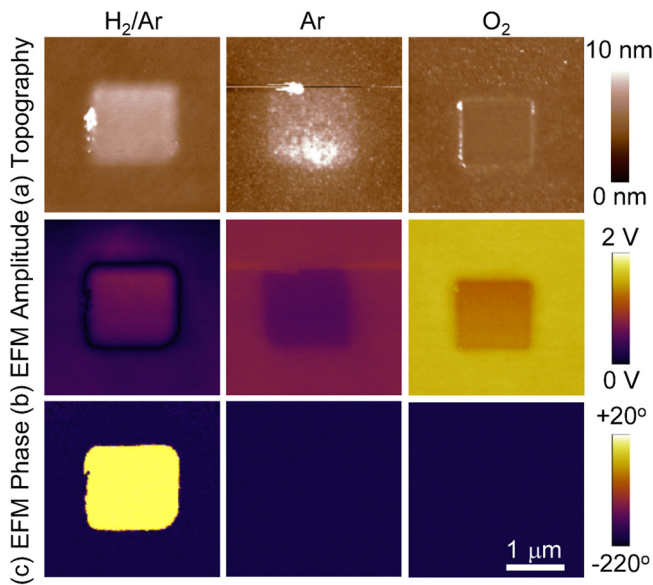


FIG. 1. (Color online) (a) Topography, (b) EFM amplitude, and (c) EFM phase after the tip-induced stress over a square-shaped region of $1.5 \mu\text{m} \times 1.5 \mu\text{m}$ at the central region in H_2/Ar , Ar, and O_2 ambient.

The amplitude of the first harmonic component in F_e , $F_{1\omega}$, can be expressed as⁶

$$F_{1\omega} = \left[\frac{\partial C}{\partial z} (V_{\text{dc}} - V_{\text{surf}}) \right] V_{\text{ac}} \sin \omega t, \quad (1)$$

where V_{dc} is the DC bias voltage that is applied to the SPM tip, V_{surf} is the surface potential of the sample, z is the tip-sample separation, and C is the tip-surface capacitance. The amplitude of $F_{1\omega}$ and the phase difference between $F_{1\omega}$ and the AC modulation signal ($V_{\text{ac}} \sin \omega t$) will be termed the “EFM amplitude” and the “EFM phase,” respectively.

Figure 1(b) shows that the EFM amplitude in the stressed region is distinct from the amplitude in the unstressed region. It may also be noted that even in the unstressed region, the EFM amplitude differs depending on the atmosphere. Moreover, the EFM phase images in Fig. 1(c) show that an EFM phase of 0° occurs only in the H_2/Ar stressed region, indicating a considerable modification of V_{surf} . These results suggest that the V_{surf} of TiO_2 can be influenced both by the tip-induced stress and by the gas environment.

For further quantitative analyses, the line profiles of the EFM amplitude and phase were obtained, as shown in Fig. 2(a). The EFM amplitude of the unstressed region in the reduction ambient is smaller than that in the oxidation ambient. This observation implies that the difference in V_{surf} could be related to the amount of oxygen in the ambient, which is related to both chemical switching of ferroelectric materials⁴ and surface depletion caused by oxygen adsorption in n -type semiconducting oxides, including TiO_2 .^{8–11}

Figures 2(a) and 2(b) clearly show that the tip-induced stress modifies the EFM data and that the behaviors strongly depend on the ambient gas. The tip-induced stress decreases the EFM amplitude in Ar and O_2 , but it increases the amplitude in H_2/Ar . The EFM phase in the stressed region in H_2/Ar is 0° , and in all the other cases, this phase is -180° . Figure 2(c) illustrates the relationship between the EFM amplitude, the EFM phase, and V_{surf} , which can be inferred from Eq. (1). When V_{dc} is zero and V_{surf} is negative (positive), the EFM phase should be -180° (0°). If the magnitude of V_{surf} is varied while maintaining constant polarity, the EFM amplitude should be variable and the EFM phase should be invariant. Such a case corresponds to the middle figure in Fig. 2(c), which agrees well with the EFM results for Ar and O_2 . The last figure in Fig. 2(c) illustrates the case of polarity reversal in V_{surf} , the EFM amplitude should be zero, and the EFM phase change occurs at the location where the sign of V_{surf} is changed. This figure matches the results in H_2/Ar . Figures 2(a)–2(c) clearly reveals that the influence of the tip-induced-stress on the TiO_2 surface potential can be drastically altered by the gas ambient.

Figure 3(a) shows V_{surf} in the unstressed region for H_2/Ar , Ar, and O_2 . From Eq. (1), it can be seen that the local V_{surf} can be estimated by finding the minimum of the EFM magnitude by adjusting V_{dc} (see supplementary material for details (Ref. 15)).⁶ V_{surf} , which was obtained from such a procedure, was negative in all the gases, and became smaller when changing from a reduction to an oxidation ambient. The energy band diagram of a TiO_2 surface is schematically illustrated in Fig. 3(b). The work function of a sample, W_S , depends on several factors, such as the surface dipole energy ($\Delta\phi_S$), the surface band bending (eV_S), the electron affinity (χ), and the carrier concentration (i.e., $E_C - E_F$). These dependencies are expressed by the following equation:¹⁶

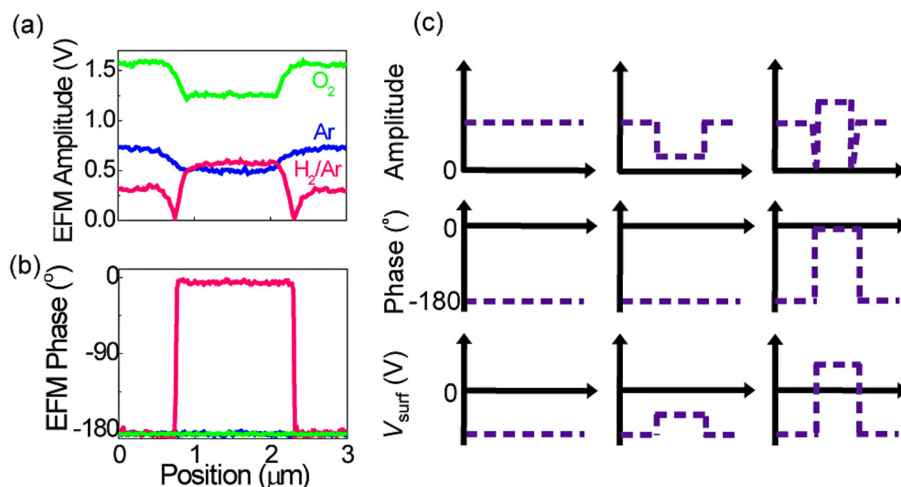


FIG. 2. (Color online) The line profiles of (a) EFM amplitude and (b) EFM phase, which were obtained from the EFM data of Fig. 1. (c) Schematic illustrations of the EFM responses for three distinct cases of spatial variation in V_{surf} ($V_{\text{dc}} = 0 \text{ V}$).

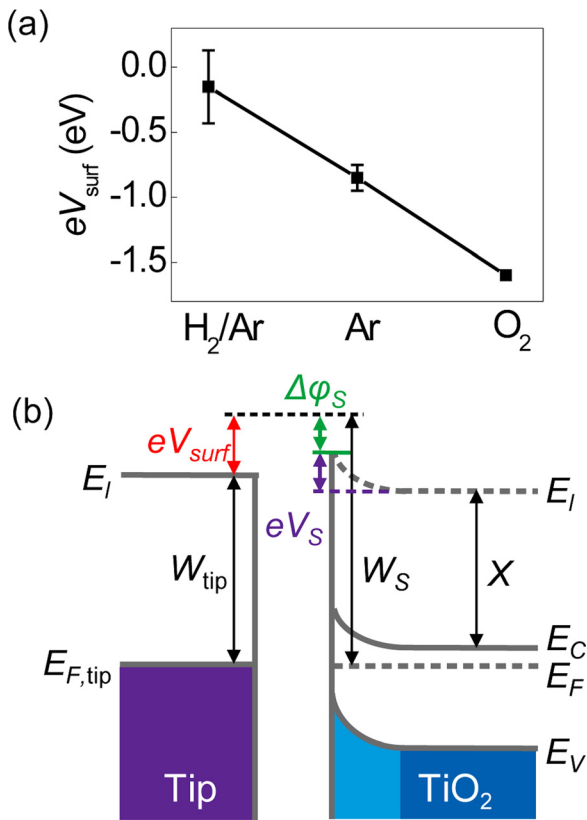


FIG. 3. (Color online) (a) V_{surf} of the unstressed TiO₂ region under various ambient conditions. (b) The schematic band diagram of a parallel-plate capacitor consisting of a metal (SPM tip) and an n-type semiconductor (TiO₂).

$$W_S = (E_C - E_F) + eV_S + \chi + \Delta\phi_S. \quad (2)$$

V_{surf} is largely dependent on the gas ambient in our results, as shown Fig. 3(a). This suggests that W_S can be dominantly affected by the adsorption effects.^{8,13} Based on the assumption that the difference between $W_S[\text{O}_2]$ and $W_S[\text{H}_2/\text{Ar}]$ is solely caused by $\Delta\phi_S$ (implying that the other factors in Eq. (2) do not make significant contributions), $\Delta\phi_S = W_S[\text{O}_2] - W_S[\text{H}_2/\text{Ar}] = -1.3$ eV. This result leads to an estimated monolayer

(ML) coverage of 3.8%, if the oxygen molecules are adsorbed on the TiO₂ and are located 2 Å above the surface. This level of oxygen adsorption is similar to the reported values of oxygen vacancy density (4.3% ML), indicating that the oxygen molecules preferably adsorb at the surface oxygen vacancy sites as in the case with TiO₂ (110) surface.¹⁰ The V_{surf} in Ar was measured at -0.85 eV, which is in between the results for H₂/Ar and O₂. All of these results suggest that the oxygen adsorption can be the dominant origin of the ambient effects on V_{surf} .⁸

Henrich *et al.* reported that the work function of TiO₂ decreased as increasing the density of defect states (mostly oxygen vacancies) through their ultraviolet photoemission spectroscopy (UPS) data and attributed such results to the change of the surface electronic structures.¹¹ In reduction ambient of H₂/Ar, the oxygen vacancy concentration on our sample surface might be somewhat larger than those in other ambient. Thus, the V_{surf} change in Fig. 3(a) can be partly caused by the electronic structural modification.

Figure 4 provides schematic diagrams illustrating our scenario for each of the EFM results. The main participants are the adsorbed oxygen ions (O₂⁻), oxygen vacancies (V_O^{••}), and holes (h⁺),⁸⁻¹¹ and they interact with the gas ambient and the biased tip as follows. The SPM-tip-induced removal of oxygen from the TiO₂ can generate an oxygen vacancy. There are few oxygen molecules adsorbed on the TiO₂ surface in H₂/Ar, and $\Delta\phi_S$ is smaller than it is in Ar and O₂. As a result, V_{surf} is larger (i.e., W_S is smaller) in H₂/Ar than it is in Ar and O₂. During the tip-induced stress, the tip can exert an attractive force on the oxygen ions (anions) in the sample. Some of the oxygen ions on the surface can escape from the surface with the aid of the huge electric field between the tip and the sample, which can be called the SPM-tip-induced surface redox phenomenon.¹⁴ This reduction should increase the TiO₂ oxygen vacancy concentration and decrease the quantity ($E_C - E_F$), resulting in an increased V_{surf} (see Eq. (2)). It is worth noting that V_{surf} was increased by $+0.30 \pm 0.18$ eV after the tip-induced stress was applied in the H₂/Ar. This result indicates that the V_{surf} polarity changed after

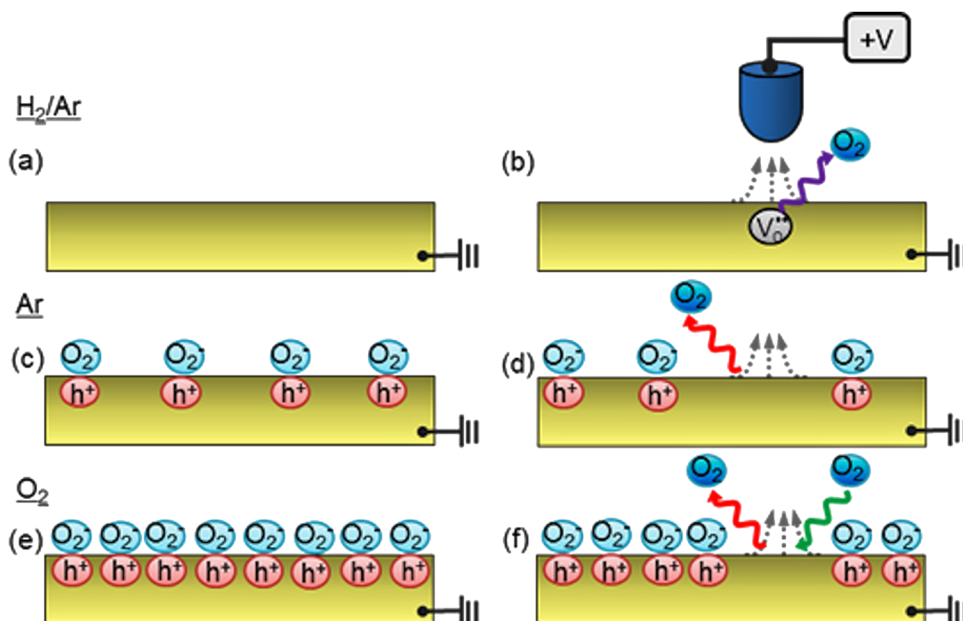


FIG. 4. (Color online) Schematic illustrations for the TiO₂ surface before the tip-induced stress in (a) H₂/Ar, (c) Ar, and (e) O₂, and during the tip-induced stress in (b) H₂/Ar, (d) Ar, and (f) O₂.

the stress, as illustrated in Fig. 2(c). If such a change is primarily caused by $\Delta(E_C - E_F)$, the number of carriers after the stress must be larger than the number before the stress by a factor of $\sim 10^4$, which may lead to drastic increase in surface charge distribution and enhanced conductivity in the oxide materials.^{2,3}

In an Ar ambient, some of the adsorbed oxygen ions at the TiO₂ surface can be desorbed during the purging of the SPM cell, due to the low partial O₂ pressure. The adsorbed oxygen molecules are not likely to be completely removed, and the V_{surf} data in Fig. 3(a) ($V_{\text{surf}}[\text{H}_2/\text{Ar}] > V_{\text{surf}}[\text{Ar}] > V_{\text{surf}}[\text{O}_2]$) are in good agreement with this expectation. The positively biased tip may help desorption of the oxygen at the TiO₂ surface, but it may not easily remove the oxygen from the bulk of the TiO₂.^{3,14} As discussed above, and as illustrated in Fig. 2(c), the decrease in the EFM amplitude and the invariance of the EFM phase after the tip-induced stress in Ar can be explained by the desorption of gas molecules, rather than by the removal of oxygen from the TiO₂.^{3,14}

In the case of O₂ ambient, there are sufficient supplies of oxygen molecules that can be adsorbed on the TiO₂ surface.^{8–11} A positively biased tip can remove the oxygen ions from the surface, while extracting oxygen from the inside of TiO₂ is difficult to induce.^{3,14} In the O₂, the stressed region did not show a notable change in V_{surf} after the tip-induced stress. This result supports our reasoning that the supply of oxygen from the ambient can induce continuous adsorption at the surface and compensate for the gas desorption.

As an alternative possibility, the biased tip can detach electrons as well as the oxygen ions from the sample surface. Both of the processes can lower the work function of the samples, and clear distinction may not be straightforward. Xie *et al.* performed the tip-induced stress experiments similar to us and ruled out the charge injection scenario due to the robust charge retention compared to other compound semiconductor samples.² However, we can qualitatively compare the effects of charge injection and oxygen desorption from Fig. 2(a). If the charge injection is the main mechanism of changing the surface potential, the oxygen anion will be attracted more to the surface contributing to higher EFM amplitude. However, as seen in Fig. 2(a), the tip-induced stress resulted in decrease in the EFM amplitude and even a phase reversal in H₂/Ar. This shows that the oxygen desorption is the main mechanism for the change in the surface potential of TiO₂ single crystal. Furthermore, surface potential changed even in the regions where no tip-induced stress was applied as seen in the regions outside the square in Fig. 1 and plotted in Fig. 3(a). The surface potential change by different gas environment can only be explained by oxygen desorption. In addition, the observed surface potential

difference after the tip-induced stress exhibited strong ambient dependence, which may not be readily explained by the charge injection process.

In conclusion, the surface potential of the TiO₂ single crystals that were scanned by a positively biased tip, as revealed by EFM, showed a polarity reversal only in the reduction atmosphere supplied by H₂/Ar. Such results indicate that the reduction ambient and resulting amount of O₂ adsorbates on the surface play key roles in determining the TiO₂ surface potential after the biased tip scanning. Through quantitative analyses, it was found that the distribution of the charges (both the charges adsorbed at the surface and the constituent ones in the sample) should be considered when explaining the EFM results.

H.K. and D.-W.K. were supported by the Quantum Metamaterials Research Center (2009-0063324) and the Basic Research Program (2010-0009344) through the National Research Foundation of Korea Grant funded by the Korean Ministry of Education, Science, and Technology. The SPM experiments and data analysis (H.K. and S.H.) were conducted at the Materials Science Division of Argonne National Laboratory, a U.S. DOE Office of Science Laboratory, operated under Contract No. DE-AC02-06CH11357.

¹C. H. Ahn, J. M. Triscone, and J. Mannhart, *Nature* **424**, 1015 (2003).

²Y. W. Xie, C. Bell, T. Yajima, Y. Hikita, and H. Y. Hwang, *Nano Lett.* **10**, 2588 (2010).

³F. Bi, D. F. Bogorin, C. Cen, C. W. Bark, J.-W. Park, C.-B. Eom, and J. Levy, *Appl. Phys. Lett.* **97**, 173110 (2010).

⁴M. J. Highland, T. T. Fister, M.-I. Richard, D. D. Fong, P. H. Fuoss, C. Thompson, J. A. Eastman, S. K. Streiffer, and G. B. Stephenson, *Phys. Rev. Lett.* **105**, 167601 (2010).

⁵H. Ko, K. Ryu, H. Park, C. Park, D. Jeon, Y. K. Kim, J. Jung, D.-K. Min, Y. Kim, H. N. Lee, Y. Park, H. Shin, S. Hong, *Nano Lett.* **11**, 1428 (2011).

⁶S. Hong, J. Woo, H. Shin, J. U. Jeon, Y. E. Pak, E. L. Colla, N. Setter, E. Kim, and K. No, *J. Appl. Phys.* **89**, 1377 (2001).

⁷D. B. Strukov, G. S. Snider, D. R. Stewart, and R. S. Williams, *Nature* **453**, 80 (2008).

⁸W. Gopel, *Prog. Surf. Sci.* **20**, 9 (1985).

⁹V. E. Henrich and P. A. Cox, *The Surface Science of Metal Oxides* (Cambridge University Press, Cambridge, 1994).

¹⁰C. M. Yim, C. L. Pang, and G. Thornton, *Phys. Rev. Lett.* **104**, 036806 (2010).

¹¹V. E. Henrich, G. Dresselhaus, and H. J. Zeiger, *Phys. Rev. Lett.* **36**, 1335 (1976).

¹²R. W. Li, T. Kanki, M. Hirooka, A. Takagi, T. Matsumoto, H. Tanaka, and T. Kawai, *Appl. Phys. Lett.* **84**, 2670 (2004).

¹³D. Li, M. H. Zhao, J. Garra, A. M. Kolpak, A. M. Rappe, D. A. Bonnell, and J. M. Vohs, *Nat. Mater.* **7**, 473 (2008).

¹⁴A. Kumar, F. Ciucci, A. N. Morozovska, S. V. Kalinin, and S. Jesse, *Nat. Chem.* **3**, 707 (2011).

¹⁵See supplementary material at <http://dx.doi.org/10.1063/1.3675630> for details on experimental procedures.

¹⁶A. Rothschild, A. Levakov, Y. Shapira, N. Ashkenasy, and Y. Komem, *Surf. Sci.* **532–535**, 456 (2003).